HHS Public Access

Author manuscript

J Inorg Biochem. Author manuscript; available in PMC 2023 January 11.

Published in final edited form as:

J Inorg Biochem. 2022 September ; 234: 111877. doi:10.1016/j.jinorgbio.2022.111877.

Fluorescent Half-Sandwich Iridium Picolinamidate Complexes for In-Cell Visualization

Sohini Bose[a], **Hieu D. Nguyen**[a], **Anh H. Ngo**[a], **Loi H. Do**[a,*]

[a]Department of Chemistry, University of Houston, Houston, Texas 77004, United States

Abstract

In this work, we report on the development of fluorescent half-sandwich iridium complexes using a fluorophore attachment strategy. These constructs consist of pentamethylcyclopentadienyl (Cp*) iridium units ligated by picolinamidate donors conjugated to green-emitting boron-dipyrromethene (bodipy) dyes. Reaction studies in H_2O/THF mixtures showed that the fluorescent Ir complexes were active as catalysts for transfer hydrogenation, with activities similar to that of their non-fluorescent counterparts. The iridium complexes were taken up by NIH-3T3 mouse fibroblast cells, with 50% inhibition concentrations ranging from ~20-70 μM after exposure for 3 h. Visualization of the bodipy-functionalized Ir complexes in cells using fluorescence microscopy revealed that they were localized in the mitochondria and lysosome but not the nucleus. These results indicate that our fluorescent iridium complexes could be useful for future biological studies requiring intracellular catalyst tracking.

Graphical Abstract

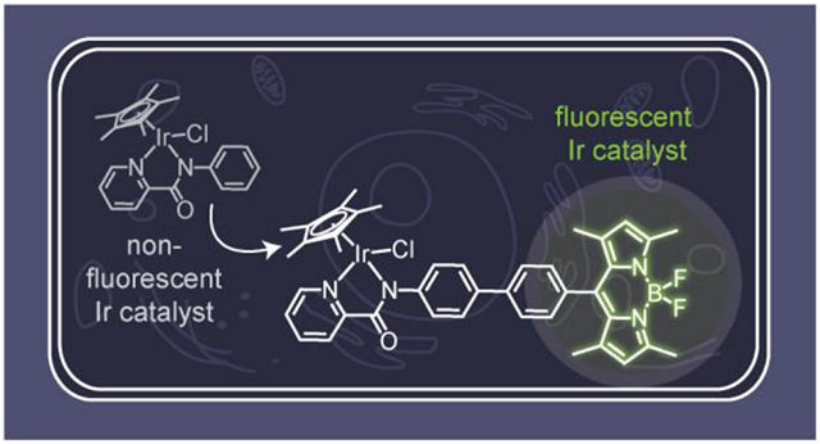

Keywords

Iridium; Half-Sandwich Complexes; Fluorescence; Transfer Hydrogenation

*Corresponding author, loido@uh.edu (L. H. Do).

Declaration of Competing Interest

The authors declare that they have no known competing financial interests or personal relationships that could have appeared to influence the work reported in this paper.

1. Introduction

Half-sandwich metal complexes have been studied extensively for their potential therapeutic properties and unique modes of action.[1–3] A variety of promising candidates have been found to be potent against platinum-drug resistant cancer cells and can interact with non-nucleic acid targets. Some studies have shown that half-sandwich metal complexes could engage in catalytic reactions inside living cells,[4–7] such as those that promote allyl carbamate cleavage[8,9] or transfer hydrogenation processes.[10–12] These complexes are currently being explored as potential catalytic drugs.

Our laboratory is interested in the development of half-sandwich metal complexes as reductase enzyme mimics.[13] These small-molecule intracellular metal catalysts (SIMCats)[6] can facilitate the conversion of carbonyl-containing compounds into their alcohol products using reduced nicotinamide adenine dinucleotide or sodium formate as the hydride source. This reaction could be useful for detoxifying α,β-unsaturated aldehydes that are associated with neurodegenerative disorders, cancers, atherosclerosis, and other oxidative stress-related diseases.[14–17] A systematic study of pentamethylcyclopentadienyl (Cp*) iridium complexes revealed that the identity of their bidentate supporting ligand is critical to their transfer hydrogenation behavior under biologically relevant conditions.[18,19] For example, Cp*Ir species ligated by 2,2′-bipyridine or 2-phenylpyridine were catalytically inactive, whereas those ligated by electron-rich picolinamidate donors showed excellent activity. Excitingly, these iridium complexes were able to convert aldehydes to alcohols inside live mammalian cells, which was established using a turn-on fluorescent substrate strategy.[11] Unfortunately, because these iridium complexes are non-fluorescent, it was not possible to visualize their intracellular distribution or measure their reaction kinetics on a single cell level. This information would be useful to determine what percentage of the Ir complexes are active inside cells and whether their catalytic behavior is cell location dependent. Such knowledge would aid in the design of SIMCats with improved biocompatibility and efficiency.

A common strategy to make non-fluorescent metal complexes emissive is to append organic fluorophores to their ligand structures (Scheme 1).[23–28] This method has been used successfully to create a variety of fluorescent Cp*Ir complexes. For example, Sierra and coworkers attached boron dipyrromethene (bodipy) groups to [IrCl(η^5-Cp*)(2-ppy)] (2-ppy = 2-phenylpyridine) complexes.[20,29] They observed that the distance between the bodipy fluorophore and the metal center had a significant impact on the complex's emission properties. A photoinduced electron transfer quenching mechanism was proposed to be responsible for the non-emissive character of Ir species with short metal-fluorophore distances. In other examples, fluorescent [Ir(bpy)Cl(η^5-Cp*)]Cl (bpy = 2,2′-bipyridine) and [IrCl(η^5-Cp*)(PI)] (PI = 2-phenoxyimine) complexes were prepared by covalently linking rhodamine (Irrhodamine)[21] and coumarin (Ir-coumarin)[22] dyes to their ligand framework, respectively. Both Ir-rhodamine and Ir-coumarin species were visualized in cells by fluorescence microscopy and showed promising anti-cancer activity.

To the best of our knowledge, fluorescent [IrCl(η^5-Cp*)(PA)] (PA = picolinamidate) complexes have not yet been reported. Because they are among the most active catalysts in the Cp*Ir family,[18,19] we wanted to create emissive variants of this series to be used

for future in-cell reaction studies. We report in the following work our successful efforts to synthesize, characterize, and study the fluorescence properties of [IrCl(η^5-Cp*)(PA)] species tethered to green-emitting bodipy dyes.[20,24,26,27] Being able to visualize the iridium complexes using microscopy allowed us to investigate their cellular distribution and uptake properties, which is important for understanding their biological behavior.

2. Results and Discussion

2.1. Synthesis and Characterization of Ir Complexes.

The parent [IrCl(η^5-Cp*)(PA)] complexes (**Ir1a-Ir3a**, R = H, CF_3, and NMe_2, respectively) were prepared according to literature procedures (Scheme 2A).[19] To obtain their fluorescent analogues, we carried out the synthetic sequence shown in Scheme 2B. The boronic acid functionalized bodipy **2**[30] and a picolinamide precursor **4** were subjected to Suzuki-Miyaura cross-coupling using $Pd(OAc)_2$, PPh_3, and Cs_2CO_3. The desired picolinamidebodipy **4a-4c** (where R = H, CF_3, and NMe_2, respectively) were isolated in modest yields ranging from 32-37%. To metalate the ligands, **4a-4c** were treated with $[IrCl_2(\eta^5\text{-Cp*})]_2$, followed by the addition of NH_4PF_6, to afford the corresponding Ir complexes **Ir1b-Ir3b** in 47-59% yield after purification by silica gel column chromatography. All the Ir-bodipy complexes were characterized by NMR spectroscopy, which showed chemical shifts consistent with differences in their electronic structures. For example, their 2-pyridyl hydrogen peaks appeared at 8.08 (Figure S38), 8.59 (Figure S31), and 8.77 (Figure S34) ppm for **Ir3b**, **Ir1b**, and **Ir2b**, respectively, which correspond to the expected electron donation trend NMe_2 > H > CF_3. Furthermore, the *m/z* molecular ions for the $[M\text{-}Cl]^+$ species were detected by electrospray ionization mass spectrometry (Figure S43). Although the X-ray crystallographic data of these Cp*Ir(picolinamidate) species were not obtained, they are presumed to adopt typical piano-stool structures.[18,31,32]

We observed that our Ir-bodipy complexes exhibited similar spectral features (Figure S1). For example, the UV-vis absorption spectra of **Ir1b-Ir3b** showed prominent peaks with λ_{max} = ~270 and 500 nm. Excitation of the Ir complexes at 488 nm produced emission spectra with λ_{em} = ~512 nm, which is characteristic of compounds containing the bodipy chromophore.[20,27] We found that unsubstituted **Ir1b** had a slightly higher quantum yield (Φ = 0.04) than its electron-poor **Ir2b** and electronic-rich **Ir3b** derivatives (Φ = 0.02 for both). To determine whether the spectral properties of Ir-bodipy are impacted by the presence of biomolecules, we measured the emission spectra of **Ir3b** in combination with glutamine, glucose, lysine, arginine, glycine and reduced glutathione, which are components typically found in commercial cell culture media (Figure S42). We observed that the addition of glutamine, glucose, or glycine to **Ir3b** had negligible effects on the emission spectra. However, the introduction of lysine, arginine, or reduced glutathione decreased the fluorescence intensity by up to ~15%.

2.2. Transfer Hydrogenation Studies.

With the Ir complexes in hand, we proceeded to test their catalytic efficiency in promoting transfer hydrogenation. The reactions were performed by combining benzaldehyde (1 equiv.), sodium formate (3 equiv.), and Ir catalyst (0.01 equiv.) in H_2O/THF mixtures at

37 °C for 24 h. The ratio of H_2O/THF used ranged from 1.5:1.0 to 2.0:2.1, depending on the solubility of the Ir complex. We found that **Ir1b** has low solubility in both organic and aqueous solvents, **Ir2b** has good solubility in organic solvents but not aqueous solvents, and **Ir3b** has good solubility in both organic and aqueous solvents. The transfer hydrogenation reactions also proceed in H_2O/DMSO mixtures. However, we preferred using H_2O/THF because homogeneous solutions containing ≥125 μM of catalyst could be prepared. In previous studies, we had determined that [IrCl(η^5-Cp*)(PA)] complexes exist in the iridium-chloride rather than the iridium-aqua form in aqueous solutions containing high chloride concentrations (e.g., in phosphate buffered saline).[19] As shown in Figure 1, the catalysts provided the transfer hydrogenation product benzyl alcohol in 68, 5, and 95% yield for **Ir1b, Ir2b**, and **Ir3b**, respectively. This reactivity trend is consistent with that observed for the parent Ir complexes **Ir1a, Ir2a**, and **Ir3a**, which gave 85, 4, and 95% yield of benzyl alcohol, respectively. We reported in previous kinetic studies that electron-poor **Ir2a** exhibited similar hydride formation rates as that of the parent **Ir1a** and electron-rich **Ir3a**.[19] However, **Ir2a** was much slower in transferring hydrides from its Ir-H species to substrates compared to that for **Ir1a** and **Ir3a**. Because attaching bodipy groups to the picolinamidate framework in **Ir1b-Ir3b** does not alter the steric or electronic environments of the Ir centers, its presence has minimal effects on catalytic activity.

2.3. Biological Cell Studies.

To determine whether the Irbodipy complexes are cell permeable, we measured the Ir concentration of NIH-3T3 cells after treatment with 5 μM of the iridium complexes for 2 h (Table S2). Analysis by inductively coupled plasma mass spectrometry (ICP-MS) revealed that cells exposed to **Ir1b, Ir2b**, and **Ir3b** contained 179, 8, and 111 ng Ir/10^6 cells, respectively. The low cellular uptake of **Ir2b** was attributed to its poor solubility in aqueous mixtures. To assess whether the presence of the bodipy group has any effects on cell permeability, we also determined the Ir content in cells incubated with the non-fluorescent catalysts. We observed that samples in the **Ir1a, Ir2a**, and **Ir3a** control groups had concentrations of 42, 104, and 21 ng Ir/10^6 cells, respectively. Based on the results for **Ir1a** vs. **Ir1b** and **Ir3a** vs. **Ir3b**, the addition of bodipy to the Ir catalysts seemed to have increased their ability to be taken up inside cells.[33]

Next, we determined the 50% inhibition concentrations (IC_{50}) of the Ir complexes to assess their biocompatibility. To perform these experiments, NIH-3T3 cells were exposed to various concentrations of the Ir complexes for 3 h and then their cell viability was measured using colorimetric MTS assays (Table S2). Our results showed that the fluorescent **Ir1b, Ir2b**, and **Ir3b** complexes had IC_{50} values of 23, 67, and 28 μM, respectively. For comparison, the non-fluorescent **Ir1a-Ir3a** complexes gave IC_{50} values ranging from 31-119 μM. Interestingly, a plot of the cellular uptake concentrations vs. IC_{50} values revealed a general correlation between these two parameters (Figure 2). These results are consistent with other studies showing that more lipophilic complexes are better taken up by cells and tends to be more cytotoxic.[33] Although the specific biological modes of action may differ for different half-sandwich metal complexes, some possibilities include binding to proteins,[2] disrupting cellular redox homoeostasis,[5] or inhibiting enzyme function.[34] The precise mechanisms of cytotoxicity by the [IrCl(η^5-Cp*)(PA)] complexes have not yet been

fully elucidated[31] and will be the subject of future investigations. However, the present work indicates that our Ir-bodipy complexes could be well tolerated by NIH-3T3 cells at concentrations below ~20 μM (i.e., the IC_{50} value of the most cytotoxic complex in the series).

2.4. Fluorescence Cell Imaging Studies.

After establishing that our Ir-bodipy complexes are emissive and biocompatible, we next conducted fluorescence microscopy experiments to visualize the Ir complexes inside live NIH-3T3 cells. For these imaging studies, cells were grown in 8-well microscope plates and incubated with 5 μM of the iridium complex for 1 h. The cell samples were also co-treated with Mito-ID Red, Lyso-ID Red, and/or Hoechst 3342 to stain their mitochondria, lysosome, and nucleus, respectively. To minimize background fluorescence, the cells were washed with fresh phenol-free DMEM prior to imaging. Finally, the images were acquired using an Olympus IX83 microscope equipped with a 100× oil objective. Our imaging results (Figures S2–4) indicated that **Ir1b, Ir2b**, and **Ir3b** could be clearly detected inside live cells. For example, wells exposed to **Ir3b** showed strong emission emanating from the interior of the cell (Figure 3A). Two-channel imaging revealed that the Ir-bodipy complexes accumulated in both the mitochondria and lysosome. Based on the shape and morphologies of the cells, they were not adversely affected by the Ir complexes under imaging conditions. An important point to note in our studies is that the addition of a fluorophore to the Ir species could potentially alter their intracellular distribution relative to that of their parent complexes. Such possibilities could be evaluated by obtaining data from high-resolution quantitative elemental mapping of live cells treated with either emissive or non-emissive iridium variants to determine whether there are differences in their cellular distribution.[35] In this study, we did not perform experiments using less than 5 μM of the Ir-bodipy complexes, which is at least 4.6× below their IC_{50} values (Table S2), but we expect that they should be detectable at lower concentrations by our fluorescence microscope. Future work will focus on assessing the detection limit so that this information could be used for studying concentration-dependent behavior inside living cells.

The fluorescent **Ir1b, Ir2b**, and **Ir3b** complexes appeared to have similar spatial distributions inside the cell. Using our fluorescence data, we calculated the Pearson's correlation coefficient (PCC) for the Ir complexes with different cellular organelles (Figure 3B).[36] The PCC for **Ir1b, Ir2b**, and **Ir3b** were 0.74, 0.54, and 0.69 in the mitochondria, and 0.77, 0.43, and 0.68 in the lysosome, respectively. These values suggest that the Ir complexes accumulate inside both organelles, which has been observed for other related complexes.[22,37] For all Ir-bodipy species, the PCC in the nucleus is 0, indicating that they do not penetrate the nuclear membrane. Because our Ir-bodipy complexes were not designed with organelle targeting in mind, it was not surprising that they lacked cell location specificity. However, we expect that such selectivity could be achieved by appending the appropriate organelle targeting moiety to the catalyst structure.[38]

3. Conclusions

Given that the [IrCl(η^5-Cp*)(PA)] complexes are among some of the most active biocompatible transfer hydrogenation catalysts reported, we wanted to develop fluorescent variants that could be useful for future biological studies. To make the non-fluorescent Ir complexes emissive, we covalently attached bodipy fluorophores to their ligand structures. We found that this modification affected the Ir complex's water solubility but did not alter their intrinsic transfer hydrogenation activity. In solution studies, the Ir complexes catalyzed the reduction of benzaldehyde to benzyl alcohol in the presence of sodium formate and showed the relative trend: **Ir3b** (R = NMe_2) > **Ir1b** (R = H) > **Ir2b** (R = CF_3), which was consistent with the electronic effects of their different R groups. We found that the Ir-bodipy complexes have IC_{50} values ranging from ~20-70 μM and cytotoxicity is correlated with intracellular Ir concentrations. Finally, fluorescence imaging studies showed that **Ir1b, Ir2b**, and **Ir3b** are strongly emissive inside live NIH-3T3 cells with co-localization in the mitochondria and lysosome but not the nucleus. This work suggests that fluorescent Ir-bodipy complexes retain the chemical function of their parent catalyst but have the added feature of being trackable inside live cells. Most importantly, having an electronically varied series of emissive [IrCl(η^5-Cp*)(PA)] complexes will enable us to compare the intracellular reactivity of this family of catalysts for the first time using fluorescence-based methods.

Supplementary Material

Refer to Web version on PubMed Central for supplementary material.

Acknowledgements

The authors are grateful to the Welch Foundation (Grant No. E-1894) and the National Institute of General Medical Sciences of the National Institutes of Health (Grant No. R01GM129276) for funding this work. We thank Dat Nguyen for assisting with Matlab analysis, Dr. Guangjie Yan for help with imaging studies, and Prof. Tai-Yen Chen for allowing us to use his microscope.

References

(1). Gasser G; Ott I; Metzler-Nolte N Organometallic Anticancer Compounds. J. Med. Chem 2011, 54, 3–25. [PubMed: 21077686]

(2). Sullivan MP; Holtkamp HU; Meier SM; Hartinger CG Chapter Ten - The Analysis of Therapeutic Metal Complexes and Their Biomolecular Interactions. In Inorganic and Organometallic Transition Metal Complexes with Biological Molecules and Living Cells', Lo KK-W, Ed.; Academic Press: 2017, p 355–386.

(3). Steel TR; Walsh F; Wieczorek-Błauż A; Hanif M; Hartinger CG Monodentately-coordinated bioactive moieties in multimodal half-sandwich organoruthenium anticancer agents. Coord Chem. Rev 2021, 439, 213890.

(4). Soldevila-Barreda JJ; Metzler-Nolte N Intracellular Catalysis with Selected Metal Complexes and Metallic Nanoparticles: Advances toward the Development of Catalytic Metallodrugs. Chem. Rev 2019, 119, 829–869. [PubMed: 30618246]

(5). Soldevila-Barreda JJ; Sadler PJ Approaches to the Design of Catalytic Metallodrugs. Curr. Opin. Chem. Biol 2015, 25, 172–183. [PubMed: 25765750]

(6). Ngo AH; Bose S; Do LH Intracellular Chemistry: Integrating Molecular Inorganic Catalysts with Living Systems. Chem. Eur. J 2018, 24, 10584–10594. [PubMed: 29572980]

(7). Sasmal PK; Streu CN; Meggers E Metal Complex Catalysis in Living Biological Systems. Chem. Commun 2013, 49, 1581–1587.

(8). Paprocka R; Wiese-Szadkowska M; Janciauskiene S; Kosmalski T; Kulik M; Helmin-Basa A Latest developments in metal complexes as anticancer agents. Coord. Chem. Rev 2022, 452, 214307.

(9). Völker T; Meggers E Chemical Activation in Blood Serum and Human Cell Culture: Improved Ruthenium Complex for Catalytic Uncaging of Alloc-Protected Amines. ChemBioChem 2017, 18, 1083–1086. [PubMed: 28425643]

(10). Coverdale JPC; Romero-Canelón I; Sanchez-Cano C; Clarkson GJ; Habtemariam A; Wills M; Sadler PJ Asymmetric Transfer Hydrogenation by Synthetic Catalysts in Cancer Cells. Nat. Chem 2018, 10, 347–354. [PubMed: 29461524]

(11). Bose S; Ngo AH; Do LH Intracellular Transfer Hydrogenation Mediated by Unprotected Organoiridium Catalysts. J. Am. Chem. Soc 2017, 139, 8792–8795. [PubMed: 28613857]

(12). Infante-Tadeo S; Rodríguez-Fanjul V; Habtemariam A; Pizarro AM Osmium(ii) tethered half-sandwich complexes: pH-dependent aqueous speciation and transfer hydrogenation in cells. Chem. Sci 2021, 12, 9287–9297. [PubMed: 34349898]

(13). McMahon RE Enzymatic Oxidation and Reduction of Alcohols, Aldehydes and Ketones. In Concepts in Biochemical Pharmacology: Part 2; Brodie BB, Gillette JR, Ackerman HS, Eds.; Springer Berlin Heidelberg: Berlin, Heidelberg, 1971, p 500–517.

(14). Schauenstein E; Esterbauer H; Zollner H Aldehydes in Biological Systems: Their Natural Occurances and Biological Activities; Pion Limited: London, 1977.

(15). Bradley MA; Xiong-Fister S; Markesbery WR; Lovell MA Elevated 4-Hydroxyhexenal in Alzheimer's Disease (AD) Progression. Neurobiol. Aging 2012, 33, 1034–1044. [PubMed: 20965613]

(16). Dalleau S; Baradat M; Guéraud F; Huc L Cell Death and Diseases Related to Oxidative Stress: 4-Hydroxynonenal (HNE) in the Balance. Cell Death Differ. 2013, 20, 1615–1630. [PubMed: 24096871]

(17). Lee SE; Park YS Role of Lipid Peroxidation-Derived α,β-Unsaturated Aldehydes in Vascular Dysfunction. Oxid. Med. Cell Longev 2013, 2013, 1–7.

(18). Ngo AH; Ibañez M; Do LH Catalytic Hydrogenation of Cytotoxic Aldehydes Using Nicotinamide Adenine Dinucleotide (NADH) in Cell Growth Media. ACS Catal. 2016, 6, 2637–2641.

(19). Ngo AH; Do LH Structure–Activity Relationship Study of Half-Sandwich Metal Complexes in Aqueous Transfer Hydrogenation Catalysis. Inorg. Chem. Front 2020, 7, 583–591.

(20). Chu GM; Fernández I; Guerrero-Martínez A; Ramírez de Arellano C; Sierra MA Fluorescence Quenching in BODIPYs Having Ir- and Rh-Tethered Complexes. Eur. J. Inorg. Chem 2016, 844–852.

(21). Ma W; Guo L; Tian Z; Zhang S; He X; Li J; Yang Y; Liu Z Rhodamine-Modified Fluorescent Half-Sandwich Iridium and Ruthenium Complexes: Potential Application as Bioimaging and Anticancer Agents. Dalton Trans. 2019, 48, 4788–4793. [PubMed: 30892340]

(22). Liu C; Liu X; Ge X; Wang Q; Zhang L; Shang W; Zhang Y; Yuan XA; Tian L; Liu Z; You J Fluorescent Iridium(III) Coumarin-Salicylaldehyde Schiff Base Compounds as Lysosome-Targeted Antitumor Agents. Dalton Trans. 2020, 49, 5988–5998. [PubMed: 32314774]

(23). Nazarov AA; Risse J; Ang WH; Schmitt F; Zava O; Ruggi A; Groessl M; Scopelitti R; Juillerat-Jeanneret L; Hartinger CG; Dyson PJ Anthracene-Tethered Ruthenium(II) Arene Complexes as Tools To Visualize the Cellular Localization of Putative Organometallic Anticancer Compounds. Inorg. Chem 2012, 51, 3633–3639. [PubMed: 22394115]

(24). Zimbron JM; Passador K; Gatin-Fraudet B; Bachelet C-M; Plażuk D; Chamoreau L-M; Botuha C; Thorimbert S; Salmain M Synthesis, Photophysical Properties, and Living Cell Imaging of Theranostic Half-Sandwich Iridium–4,4-Difluoro-4-bora-3*a*,4*a*-diaza-*s*-indacene (BODIPY) Dyads. Organometallics 2017, 36, 3435–3442.

(25). Du Q; Yang Y; Guo L; Tian M; Ge X; Tian Z; Zhao L; Xu Z; Li J; Liu Z Fluorescent Half-Sandwich Phosphine-Sulfonate Iridium(III) and Ruthenium(II) Complexes as Potential Lysosome-Targeted Anticancer Agents. Dyes Pigments 2019, 162, 821–830.

(26). Gupta G; Kumari P; Ryu JY; Lee J; Mobin SM; Lee CY Mitochondrial Localization of Highly Fluorescent and Photostable BODIPY-Based Ruthenium(II), Rhodium(III), and Iridium(III) Metal Complexes. Inorg. Chem 2019, 58, 8587–8595. [PubMed: 31117633]

(27). Ramos R; Gilles J-F; Morichon R; Przybylski C; Caron B; Botuha C; Karaiskou A; Salmain M; Sobczak-Thépot J Cytotoxic BODIPY-Appended Half-Sandwich Iridium(III) Complex Forms Protein Adducts and Induces ER Stress. J. Med. Chem 2021, 64, 16675–16686. [PubMed: 34761949]

(28). Miachin K; Del Solar V; El Khoury E; Nayeem N; Khrystenko A; Appelt P; Neary MC; Buccella D; Contel M Intracellular Localization Studies of the Luminescent Analogue of an Anticancer Ruthenium Iminophosphorane with High Efficacy in a Triple-Negative Breast Cancer Mouse Model. Inorg Chem 2021, 60, 19152–19164. [PubMed: 34846878]

(29). Avello MG; de la Torre MC; Guerrero-Martínez A; Sierra MA; Gomitzka H; Hemmert C Chiral-at-Metal BODIPY-Based Iridium(III) Complexes: Synthesis and Luminescence Properties. Eur. J. Inorg. Chem 2020, 4045–4053.

(30). DiCesare N; Lakowicz JR Fluorescent Probe for Monosaccharides Based on a Functionalized Boron-Dipyrromethene with a Boronic Acid Group. Tet. Lett 2001, 42, 9105–9108.

(31). Almodares Z; Lucas SJ; Crossley BD; Basri AM; Pask CM; Hebden AJ; Phillips RM; McGowan PC Rhodium, Iridium, and Ruthenium Half-Sandwich Picolinamide Complexes as Anticancer Agents. Inorg. Chem 2014, 53, 727–736. [PubMed: 24397747]

(32). Lucas SJ; Lord RM; Basri AM; Allison SJ; Phillips RM; Blacker AJ; McGowan PC Increasing Anti-Cancer Activity with Longer Tether Lengths of Group 9 Cp* Complexes. Dalton Trans. 2016, 45, 6812–6815. [PubMed: 26924272]

(33). Liu Z; Sadler PJ Organoiridium Complexes: Anticancer Agents and Catalysts. Acc. Chem. Res 2014, 47, 1174–1185. [PubMed: 24555658]

(34). Konkankit CC; Marker SC; Knopf KM; Wilson JJ Anticancer Activity of Complexes of the Third Row Transition Metals, Rhenium, Osmium, and Iridium. Dalton Trans. 2018, 47, 9934–9974. [PubMed: 29904760]

(35). Que EL; Bleher R; Duncan FE; Kong BY; Gleber SC; Vogt S; Chen S; Garwin SA; Bayer AR; Dravid VP; Woodruff TK; OHalloran TV Quantitative Mapping of Zinc Fluxes in the Mammalian Egg Eeveals the Origin of Fertilization-induced Zinc Sparks. Nat. Chem 2015, 7, 130–139. [PubMed: 25615666]

(36). Dunn KW; Kamocka MM; McDonald JH A Practical Guide to Evaluating Colocalization in Biological Microscopy. Am. J. Physiol.- Cell PH 2011, 300, C723–C742.

(37). Li J; Tian Z; Ge X; Xu Z; Feng Y; Liu Z Design, Synthesis, and Evaluation of Fluorine and Naphthyridine–Based Half-Sandwich Organoiridium/Ruthenium Complexes with Bioimaging and Anticancer Activity. Eur. J. Med. Chem 2019, 163, 830–839. [PubMed: 30579123]

(38). Qiu K; Chen Y; Rees TW; Ji L; Chao H Organelle-Targeting Metal Complexes: From Molecular Design to Bio-Applications. Coord. Chem. Rev 2019, 378, 66–86.

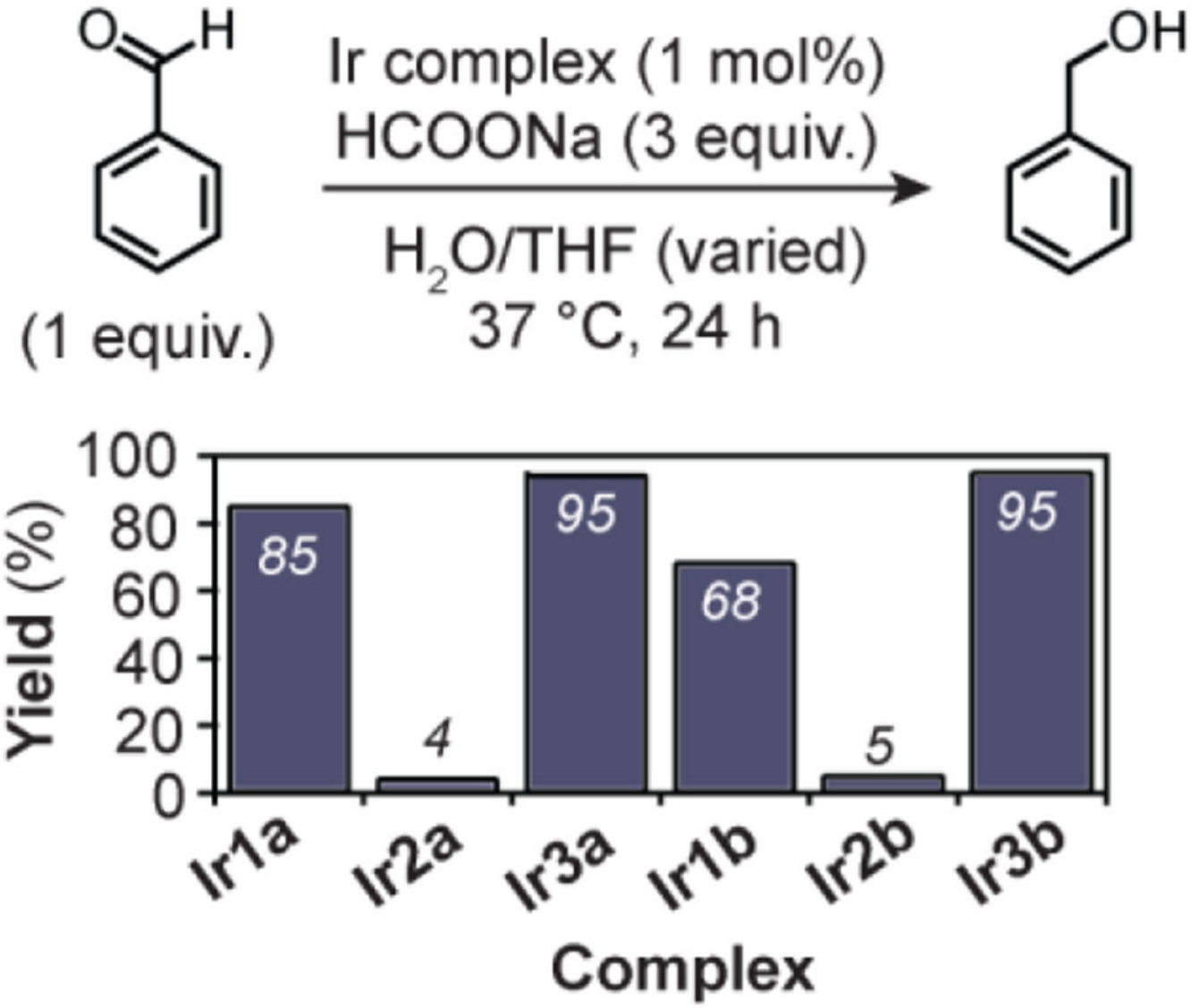

Figure 1.

Comparison of transfer hydrogenation activity in H_2O/THF solution. Reaction conditions used: benzaldehyde (60 μmol), HCOONa (180 μmol), Ir complex (0.60 μmol), H_2O/THF, 37 °C, 24 h. Slightly different H_2O/THF ratios were used due to differences in the catalyst solubility (see Table S1 for more details).

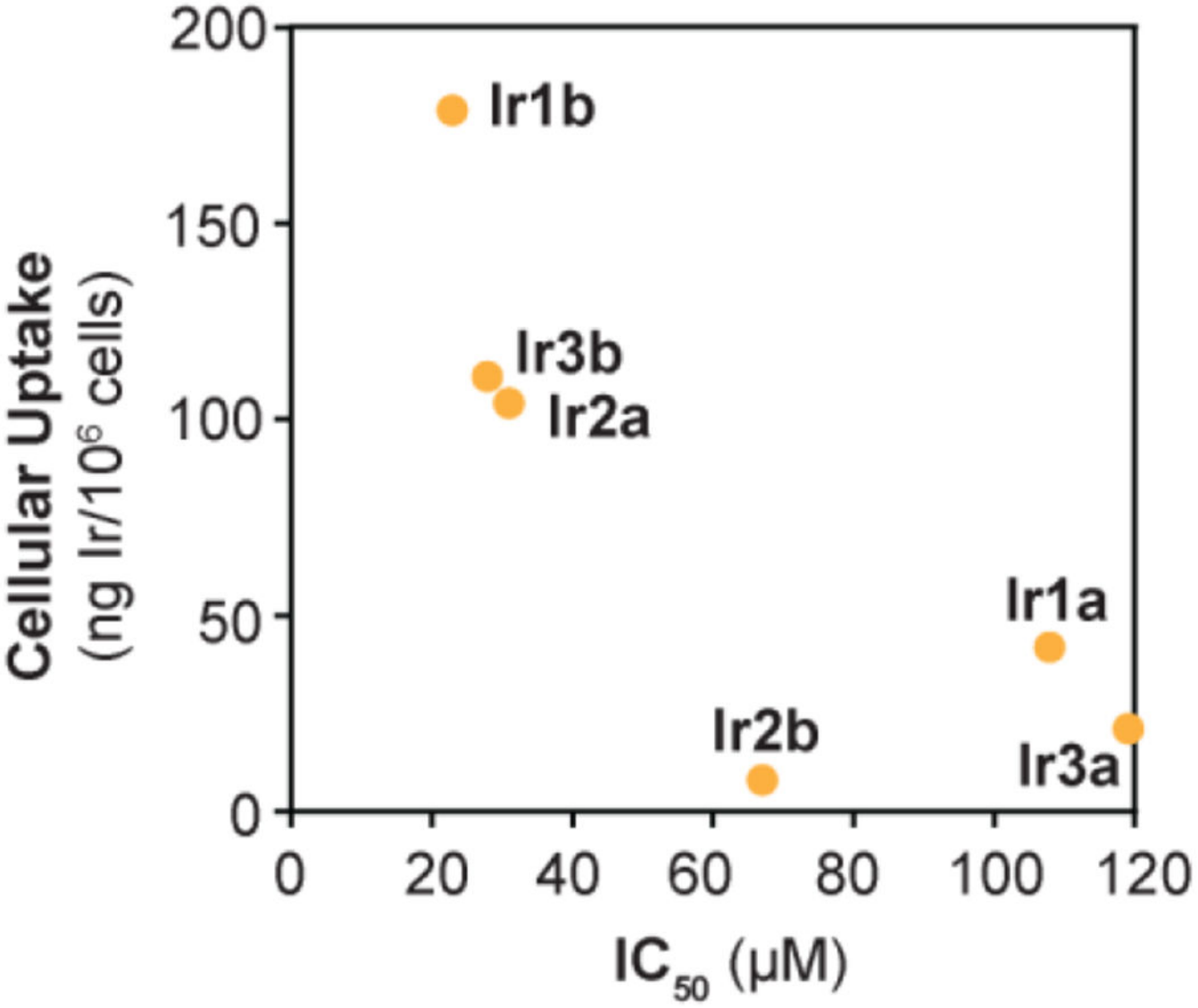

Figure 2.

Plot showing the IC_{50} concentration vs. cellular uptake of the Ir complexes. The IC_{50} values were measured using MTS assays and the cell uptake concentrations were measured by ICP-MS. See Table S2 for additional details.

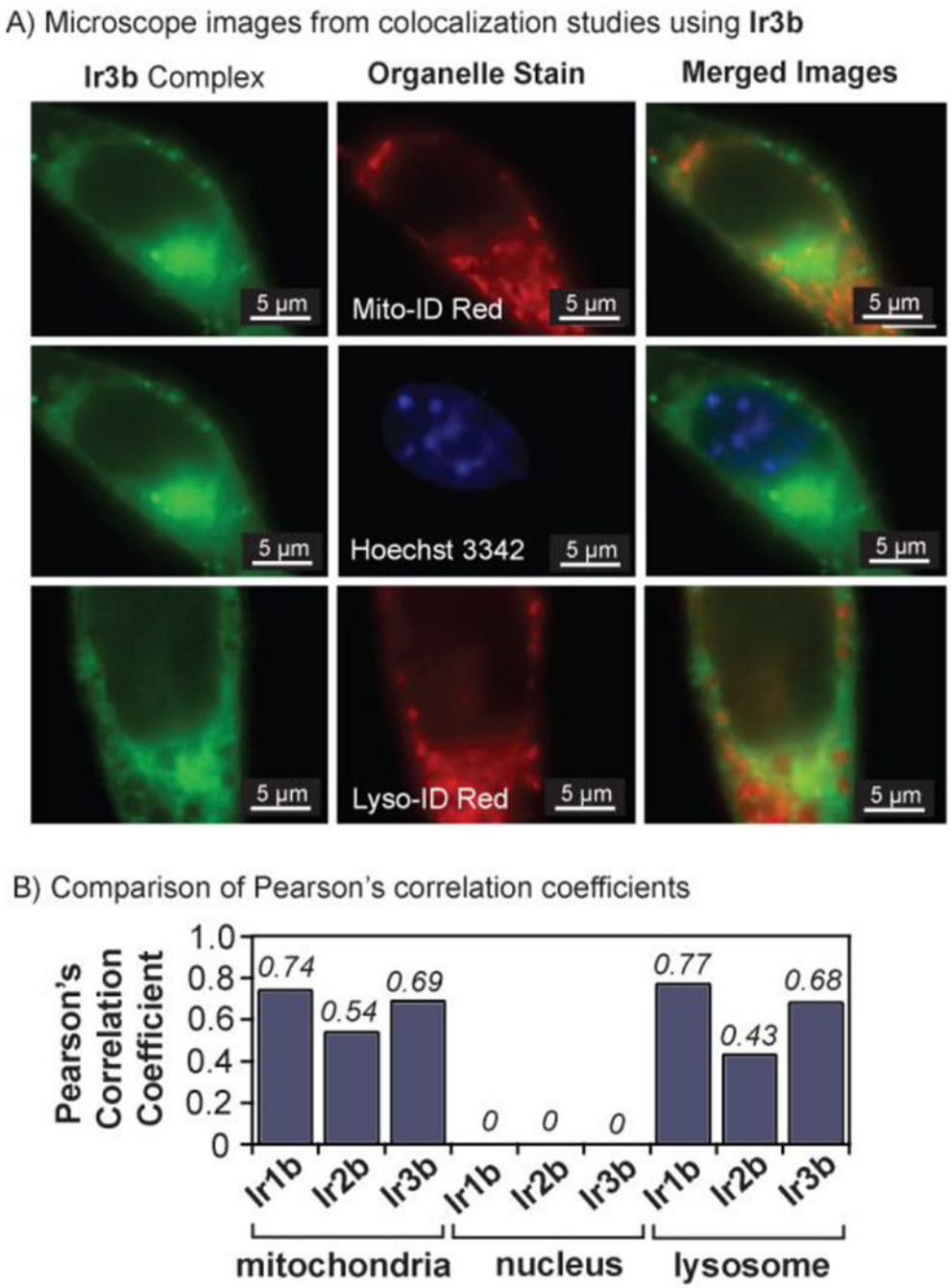

Figure 3.

A) Fluorescence microscope images of NIH-3T3 cells treated with 5 μM of **Ir3b** (λ_{ex} = 488 nm, left column) and Mito-ID Red (λ_{ex} = 561 nm channel, middle column), Hoechst 3342 (λ_{ex} = 405 nm channel, middle column), or Lyso-ID Red (λ_{ex} = 488 nm channel, middle column). The Mito-ID and Hoechst 3342 staining experiments were performed on the same cells so the top two **Ir3b** images are identical. These data were acquired using an Olympus IX83 microscope with a 100× oil objective. B) Summary of the Pearson's correlation coefficients calculated from the co-localization studies.

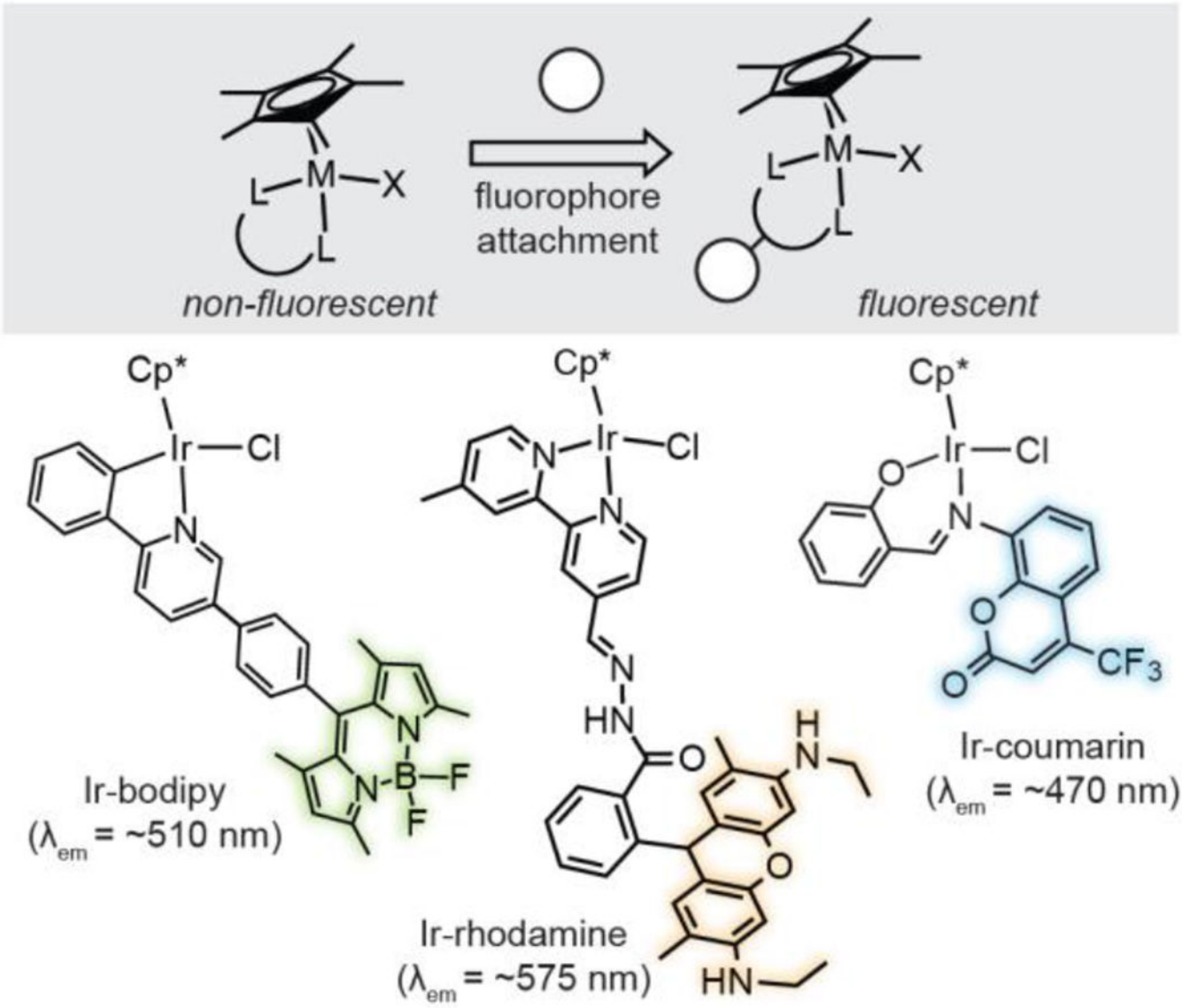

Scheme 1.

Design of fluorescent half-sandwich iridium complexes. Representative examples depicted: Ir-bodipy,[20] Ir-rhodamine,[21] and Ir-coumarin.[22]

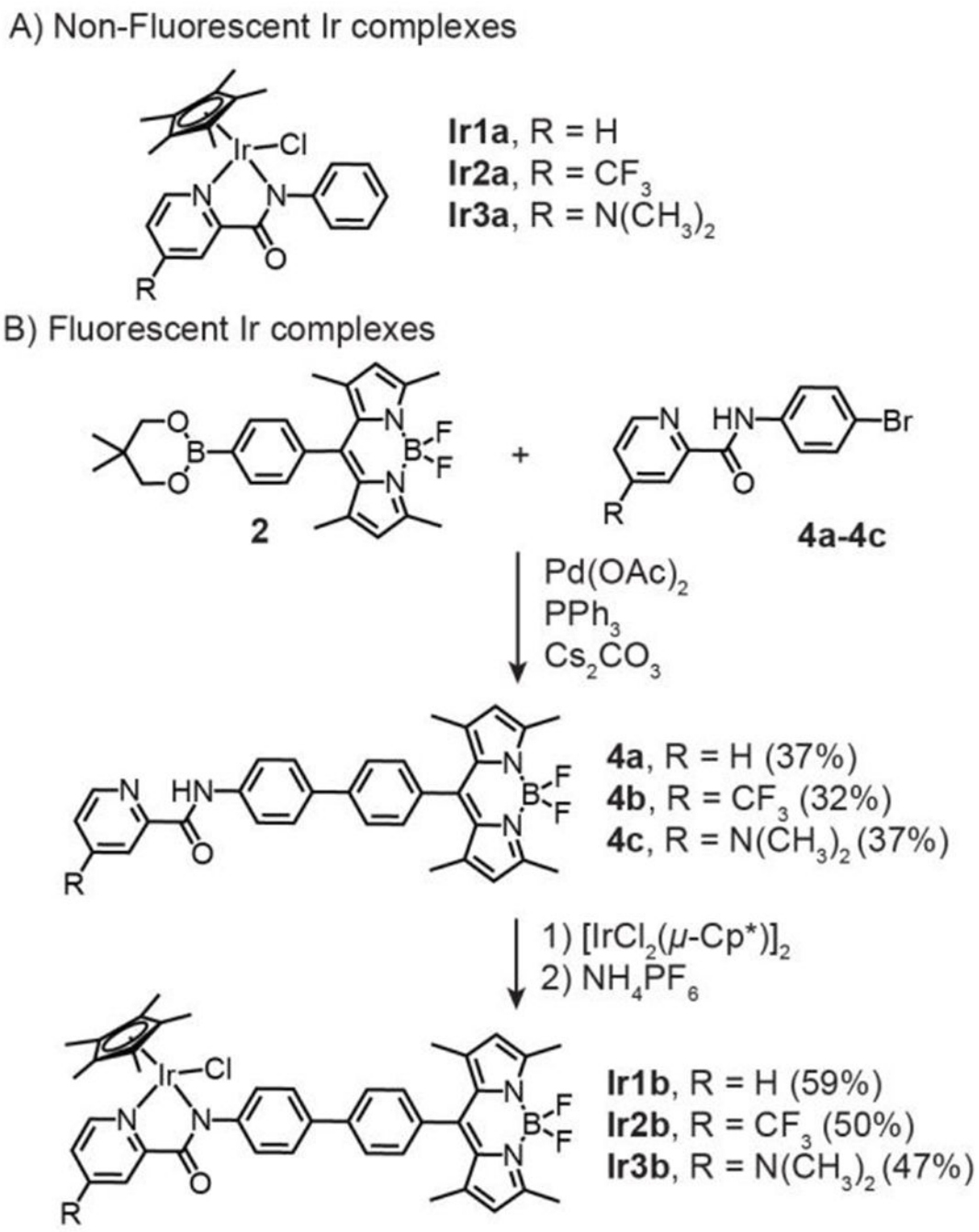

Scheme 2.

Half-sandwich Ir picolinamidate complexes used in this study. Synthesis of the fluorescent Ir complexes is shown in Part B.